The turbulent life of phytoplankton

By S. Ghosal†, M. Rogers‡ AND A. Wray‡

Phytoplankton is a generic name for photosynthesizing microscopic organisms that inhabit the upper sunlit layer (euphotic zone) of almost all oceans and bodies of freshwater. They are agents for "primary production," the incorporation of carbon from the environment into living organisms, a process that sustains the aquatic food web. It is estimated that phytoplankton contribute about half of the global primary production, the other half being due to terrestrial plants. By sustaining the aquatic food web and controlling the biogeochemical cycles through primary production, phytoplankton exert a dominant influence on life on earth. Turbulence influences this process in three very important ways. First, essential mineral nutrients are transported from the deeper layers to the euphotic zone through turbulence. Second, turbulence helps to suspend phytoplankton in the euphotic zone since in still water, the phytoplankton, especially the larger species, tend to settle out of the sunlit layers. Third, turbulence transports phytoplankton from the surface to the dark sterile waters, and this is an important mechanism of loss. Thus, stable phytoplankton populations are maintained through a delicate dynamic balance between the processes of turbulence, reproduction, and sinking. The first quantitative model for this was introduced by Riley, Stommel and Bumpus in 1949. This is an attempt to extend their efforts through a combination of analysis and computer simulation in order to better understand the principal qualitative aspects of the physical/biological coupling of this natural system.

1. Introduction

The word "plankton" comes to us (Thurman (1997)) from a Greek word ($\pi\lambda\alpha\nu\kappa\tau o\zeta$) meaning "wanderers" or "drifters" first coined by the German scientist Victor Heusen (1887). They refer to the large class of microscopic organisms (2–200 μm) that are carried around by the currents in any natural body of water. Biologists have various ways of organizing the many species of plankton into classes and subclasses¶. At the lowest level, they are divided into two classes "phytoplankton" and "zooplankton". The members of the former class photosynthesize with the help of chlorophyll and thereby contribute to primary production, the latter do not photosynthesize, but sustain themselves by "grazing" on the phytoplankton.

The distribution of phytoplankton is not uniform, but varies over large as well as small length and time scales‖. The phytoplankton density, like weather patterns, shows chaotic dynamics and is influenced by a wide range of conditions. Though a fully predictive

† Mechanical Engineering, Northwestern University
‡ NASA Ames Research Center, Moffett Field, CA

¶ Excellent illustrated compilations of plankton species exist on the internet, see e.g. http://www.calacademy.org/research/diatoms/diatoms.html.

‖ NASA's SeaWiFS project continuously provides global maps, similar to "weather maps", of the worldwide phytoplankton distribution through satellite imaging, see http://seawifs.gsfc.nasa.gov/SEAWIFS.html.

model does not seem attainable in the near future, a fundamental understanding of the basic physical processes underlying this variability is of great importance.

Because photosynthesis removes carbon dioxide from the atmosphere and releases oxygen, the global primary production due to phytoplankton is an important variable in climate models. There are also more subtle but extremely important effects on global biogeochemistry. For example, it has been suggested (Charlson *et al.* (1987)) that dimethylsulphide released by phytoplankton algae is a major source of cloud condensation nuclei. Cloud albedo is believed to be a critical factor in climate models since it controls global absorption of solar irradiance. The health of the marine system is closely linked to phytoplankton productivity, the richest fisheries tend to be concentrated in areas where upwellings bring mineral nutrients to the surface and support large phytoplankton populations. In addition to providing organic material to feed the higher animals, phytoplankton sustain aquatic life by enriching the water with oxygen, a byproduct of photosynthesis. Sudden explosions of the phytoplankton population (known as a "bloom") can have disastrous effects, especially in coastal regions. Certain species produce deadly toxins and, when present in large concentrations, they poison fish and animals higher up in the food chain. Filter feeders such as shell fish tend to concentrate these toxins in their bodies and may poison animals that feed on them (including humans). Even species that do not create toxins can kill fish populations over a wide area. The large concentrations of plankton produced during a bloom can physically clog the gills of fish, and when the plankton die after rapidly using up the mineral nutrients, their decomposing bodies deplete the water of oxygen suffocating fish that get trapped in the bloom. The large concentrations of plankton can sometimes physically color the water giving rise to the term "red tide", though HAB ("Harmful Algal Blooms") is preferred in the scientific literature†.

The large scale dynamics of plankton concentration is controlled jointly through the effects of advection by large scale flow patterns, turbulent diffusion, gravitational settling, reproduction, and loss through grazing by zooplankton, various filter feeders, and other marine animals.

Since phytoplankton convert carbon dioxide to organic material with the aid of sunlight, the reproduction rate depends directly on the rate of photosynthesis, which in turn is controlled by the light intensity. The rate of photosynthesis increases almost linearly with light intensity (Reynolds (1984)) until it saturates. A further increase in intensity results in a slight decrease in the photosynthetic rate, an effect known as "photo-inhibition". Phytoplankton, therefore, can survive and multiply only in the upper layers of oceans and lakes known as the "euphotic zone". The depth of the euphotic zone varies widely depending on water clarity, latitude, and season. For the open ocean it is often in the range of 50 to 100 meters.

After the "light climate", the most important factor in phytoplankton productivity seems to be the concentration of inorganic salts, primarily nitrates and phosphates. These salts accumulate in the deep layers of the ocean due to runoffs from land over geological time and due to the constant "rain" of dead planktonic matter from the upper productive layers. The productivity of phytoplankton is strongly constrained by the need for light, which is only available in the upper layers, and the need for mineral nutrients, available only in the deeper layers. Terrestrial plants are in a similar predicament and have evolved roots, trunks, and branches to solve their transport problem. Phytoplankton, on the other hand, rely on vertical upwelling and turbulent transport to dredge up nutrients

† Woods Hole Oceanographic Institution maintains a very informative web site on HAB s, see http://www.redtide.whoi.edu/hab.

from the deeper waters. In the ocean, a significant correlation exists between regions of high primary productivity and regions of upwelling. The carbon dioxide needed in photosynthesis is utilized from dissolved carbonates and bi-carbonates, which are plentiful and are rarely a limiting factor in primary production.

Various other factors directly or indirectly affect plankton productivity. Water temperature and salinity have a selective effect on plankton production as individual species are adapted to survive in certain optimal temperature and salinity ranges. More importantly, temperature and salinity control the stability of water columns and, therefore, the degree of turbulent mixing. Turbulent mixing in turns controls the transport of minerals and suspension of the phytoplankton in the euphotic zone; both of these physical effects are of great importance in the population dynamics of plankton.

Grazing by zooplankton is an important mechanism of loss. The phytoplankton-zooplankton coupling gives rise to a predator/prey system with well known dynamical behavior such as limit cycles and chaos (Edwards & Brindley (1999), Truscott & Brindley (1994)). Larger animals, primarily the "filter feeders" ranging from rotifers and larvae of various kinds to whales, also crop the phytoplankton stock. In shallow bays and estuaries (the San Francisco bay, for example), "benthic grazers" such as oysters that live at the bottom form a copious sink of phytoplankton (Lucas *et al.* (1999a), Lucas *et al.* (1999b), Lucas *et al.* (1998)).

2. The role of turbulence

Phytoplankton are typically about 2 to 5 percent denser than the water in which they live. In the absence of special adaptations, they would sink out of the euphotic zone. Some species have developed gas vacuoles that make them buoyant. The physical basis for the adoption of various strategies by microscopic aquatic organisms has been discussed by Alexander (1990). The two most common classes of phytoplankton are the diatoms and the dinoflagellates. The dinoflagellates are weak swimmers and swim by means of flagella, thereby counteracting the effect of gravity. The diatoms do not actively swim, but they do have a variety of adaptations to reduce the sinking speed. This, together with the fact that natural bodies of water are often turbulent, allow stable populations to exist even though each individual organism does ultimately sink out of the euphotic zone.

Suppose that each phytoplankton sinks from the surface to the bottom of the euphotic zone in a time t_s in still water, and, in a time exactly equal to t_r from birth, each organism multiplies to form new individuals. Clearly, if $t_r > t_s$, no individual can reproduce and the population cannot be sustained. If, on the other hand, the waters are turbulent, each organism may be carried either upward or downward by eddies. The mean lifetime is not changed as a result, however; there is now a wide distribution of lifetimes around the mean t_s. Thus, even if $t_r > t_s$, a significant fraction of the population gets an opportunity to reproduce, and if the resultant increase is sufficient to offset the losses, a stable population may exist. On the other hand, if $t_r < t_s$, stable populations can exist in both still waters as well as turbulent waters. However, whereas in still waters every individual would have had an opportunity to reproduce, in the turbulent case the fraction of the population with lifetime exceeding t_s would sink before reproducing. Turbulence can therefore be either a help or a hindrance in the life of phytoplankton. This depends primarily on the size of the phytoplankton species being considered. Since smaller organisms tend to both reproduce faster and sink slower, turbulence in general tends to be essential for the survival of larger species but an impediment for the smaller ones. Some very rough estimates may be made taking 50 meters as the depth of the euphotic zone. The smallest plankton have

sizes in the range of a few microns and sink at speeds (Reynolds (1984), Eppley *et al.* (1967)) of the order of 0.1 meters per day. Therefore, for these species, $t_s \sim 500$ days. The reproduction time (Reynolds (1984), Fenchel (1974)) $t_r \sim 5$ days. These species are therefore not dependent on the mechanism of turbulent suspension, and turbulence has a negative impact: it carries viable organisms to the dark aphotic zone. The largest of the phytoplankton ($\sim 200\mu m$) sink much faster at speeds ~ 20 meters per day. For these organisms, $\tau_s \sim 2.5$ days whereas $t_r \sim 5$ days. These species depend on turbulence to survive. For the same reason, turbulence is a hindrance to the dinoflagellates that are active swimmers or the negatively buoyant phytoplankton species that naturally rise to the surface due to buoyancy aids. The relative population of diatoms and dinoflagellates in the open ocean is known to be a sensitive function of the intensity of turbulence (Margalef (1978), Gibson (2000)). During periods of high winds, diatoms are found to dominate while in periods of calm, the dinoflagellates predominate. "Red Tides" which are caused by dinoflagellates are usually preceded by days of calm conditions.

In addition to its role in suspending phytoplankton, turbulence has a second important effect on plankton population dynamics. The mineral nutrients, primarily nitrates and phosphates, needed by phytoplankton are often transported from the deep aphotic layers to the euphotic zone by turbulence. In the oceans, these mineral nutrients are often depleted in the surface layers. Their concentration typically rises with depth and reaches saturation in layers that can be as much as 500 to 1000 meters below the surface (Riley *et al.* (1949)). The character of the environment in which phytoplankton live may be broadly classified as *eutrophic* or *oligotrophic*, depending on whether mineral nutrients for phytoplankton growth are plentiful or are a limiting factor in plankton population dynamics. Examples of eutrophic environments are lakes and shallow waters in tropical and temperate zones. Deep alpine lakes and deep oceans are examples of typically oligotrophic environments. Generally, clear blue waters are indicative of an oligotrophic environment whereas greenish or brownish waters are typical of an eutrophic environment. The "eutrophication" of inland waters due to runoff of phosphate and nitrate rich effluents due to human activity is an issue of great concern in contemporary ecology. In this paper we will only consider a eutrophic environment so that the maximum plankton population is light limited and depletion of mineral nutrients plays no role.

Turbulence in natural bodies of waters is to be expected since in nature turbulent flow is the rule rather than the exception. In large lakes and the open ocean, turbulence is most often driven by the breaking of surface waves. Another mechanism is the breaking of internal waves at density interfaces. Thermal and salinity gradients due to heating by the sun and/or the ebb and flow of tides can lead to convective instability that breaks into turbulence. Stable stratification can also develop during warmer months, stabilizing the surface layers against wind driven turbulence. All these geophysical processes naturally have a profound impact on the population distribution of phytoplankton. The intensity of turbulence in natural waters varies between wide limits; dissipation rates, ϵ from 2.8×10^{-7} to 47 $\mathrm{cm}^2\mathrm{s}^{-3}$, have been reported in the ocean (Peters & Marrase (2000)).

3. A simplified description

Population dynamics of phytoplankton may be described through the following simplified partial differential equation:

$$\frac{\partial \phi}{\partial t} + \mathbf{u} \cdot \nabla \phi = S\phi - v_p \frac{\partial \phi}{\partial z} + k_T \nabla^2 \phi. \tag{3.1}$$

This is a balance equation for the plankton density ϕ and may be readily derived by considering an elementary volume of liquid (much larger than the mean separation of phytoplankton though small on the scale of variation of mean fields) being advected by the mean flow $\mathbf{u}$. The random motion due to turbulence is described through the eddy diffusivity coefficient k_T. The water surface is considered at $z = 0$ and the z axis is directed downwards. The second term on the right-hand side is a result of writing the advective term as a sum of displacements due to the average fluid flow and that due to gravitational sinking of the phytoplankton with a speed v_p relative to still water. If birth and death processes are random and independent, the net source is proportional to the concentration ϕ. A reasonable model for the net growth rate is

$$S = P(I) - L \tag{3.2}$$

where $P(I)$ is the production, which in an eutrophic environment may be parametrized by the local value of the light intensity I, and L is a constant loss rate due to natural deaths and grazing by higher animals. A constant L is clearly a simplifying approximation; coupling to the zooplankton population density is neglected in this analysis. For $P(I)$ we will use the Jassby-Platt model (Jassby & Platt (1976))

$$P(I) = \frac{r+L}{2}\left[1 + \tanh\left\{\alpha\left(\frac{I}{I_c} - 1\right)\right\}\right] \tag{3.3}$$

where r, α, and I_c are parameters characterizing the photosynthetic response of the given phytoplankton species. The light intensity decays exponentially from its value at the surface I_0 so that the intensity at depth z is given by

$$I(z) = I_0 \exp(-\mu z). \tag{3.4}$$

The extinction coefficient μ is represented as the sum of a background extinction μ_0, characterizing the transparency of the water in the absence of the phytoplankton cells, and a term due to the "shading" of the phytoplankton at a given layer by those that lie above it,

$$\mu = \mu_0 + \mu_1 \int_0^z \phi \, dz. \tag{3.5}$$

The coefficient in the expression for $P(I)$ in (3.3) has been written as $(r+L)/2$ for later convenience; it is merely a constant independent of I. We will assume that α is large so that when $I = 0$, $P(I) \approx 0$, and when $I > I_c$, $P(I)$ reaches the saturation level $r + L$, so that the net growth rate is r. The photosynthetic response of many phytoplankton species have been documented. They typically increase linearly with the light intensity for low light and then rapidly saturate. A further increase in the light intensity results in a slight depression of the photosynthesis rate, an effect known as "photoinhibition". Although Eq. (3.3) ignores photoinhibition, it is a reasonably good representation of this response curve.

In this paper we will assume that the layer of water that is turbulent is infinitely thick; that is, the "turbocline" is much below the euphotic zone. Such a model certainly does not apply in all situations. The depth of the turbocline depends on the convective stability of the water column and may very well be comparable to or much shallower than the euphotic zone depth. Such a situation may give rise to very different kinds of effects than those considered in this paper. In particular, the "Sverdrup Critical Depth Model" (SCDM) may apply in determining whether phytoplankton blooms can occur (Sverdrup (1953)).

The boundary conditions for ϕ are those of no flux at the surface and vanishing plankton density deep below the euphotic zone:

$$\left[k_T \frac{d\phi}{dz} - v_p \phi\right]_{z=0} = 0 \tag{3.6}$$

$$\phi(z \to \infty) = 0. \tag{3.7}$$

It should be noted that the formulation of the problem as presented here is nonlinear, and the amplitude as well as the shape of the profile are fully determined.

4. Layer models

It is instructive to consider the limit $\alpha \to \infty$ in the above formulation. We look for steady one-dimensional solutions $\phi = \phi(z)$. In this case, the source term S is a step function

$$S = \begin{cases} r & \text{if } z < H; \\ -L & \text{if } z \geq H \end{cases} \tag{4.1}$$

where '$z = H$' is the location of the boundary of the euphotic zone. Since $I = I_c$ determines this boundary, from (3.4) and (3.5) it follows that

$$H = \frac{H_0}{1 + \sigma \int_0^H \phi \, dz} \tag{4.2}$$

where

$$H_0 \equiv \frac{1}{\mu_0} \log\left(\frac{I_0}{I_c}\right) \tag{4.3}$$

and

$$\sigma \equiv \frac{\mu_1}{\mu_0}. \tag{4.4}$$

The steady plankton density then obeys a linear one-dimensional differential equation

$$k_T \frac{d^2\phi}{dz^2} - v_p \frac{d\phi}{dz} + S(z)\phi = 0 \tag{4.5}$$

with a piecewise constant coefficient $S(z)$ given by (4.1). The boundary conditions are (3.6) and (3.7).

We do not present the details of the algebra leading up to the solution, but sketch the general procedure and present the final analytical result. In the aphotic zone ($z > H$), Eq. (4.5) allows an exponentially growing and an exponentially decaying solution; only the latter is consistent with (3.7). In the euphotic zone ($z < H$), there are two linearly independent solutions of the form $\sim \exp(mz)$ so that the general solution is a superposition of the two with unknown coefficients A and B. The boundary condition (3.6) and the requirement that both ϕ and $d\phi/dz$ be continuous across the interface $z = H$ results in three homogeneous equations for determining the three constants A, B, and the coefficient of the exponentially decaying solution in the aphotic zone, D. Nontrivial solutions can exist if and only if the discriminant of this system of three equations is zero. This is a condition for determining H and, therefore, the amplitude of the mode since the amplitude is related to H through Eq. (4.2). Physically meaningful solutions can exist if and only if the eigenvalue H is real, positive, and $H \leq H_0$. From inspection of the solvability condition, the requirement that these conditions are valid can be deduced, and this determines a critical curve in a two-dimensional parameter space defining the region in which steady one-dimensional solutions can exist.

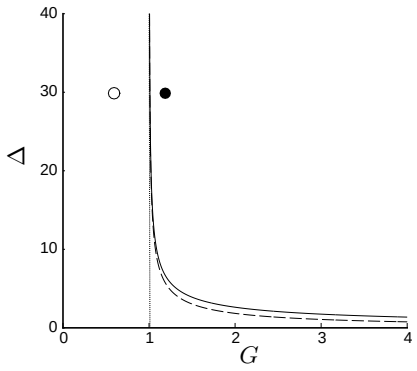

FIGURE 1. The critical curve for existence of stable populations, ——— : zero boundary condition, – – – – : no flux boundary condition. Symbols correspond to parameters for DNS.

The physical parameters characterizing the system are the net growth rate in the euphotic zone, r, the loss rate in the aphotic zone, L, the sinking speed in still water, v_p, the coefficient of turbulent diffusivity, k_T, and the clear water euphotic zone height, H_0. The analytical solution is most conveniently expressed in terms of the following two parameters, λ and Λ, with dimensions of length that determine the scale of spatial variability of the population distribution in the euphotic and aphotic zones respectively:

$$\lambda = \frac{2k_T}{v_p} \tag{4.6}$$

$$\Lambda^{-1} = \frac{v_p}{2k_T}\left[\sqrt{1+\frac{4Lk_T}{v_p^2}}-1\right]. \tag{4.7}$$

The two dimensionless parameters determining the critical curve are the dimensionless growth rate

$$G = \frac{2r\lambda}{v_p} = \frac{4rk_T}{v_p^2} \tag{4.8}$$

and the dimensionless height of the euphotic zone for clear water, Δ,

$$\Delta = \frac{H_0}{\lambda} = \frac{v_p H_0}{2k_T}. \tag{4.9}$$

The condition for existence of physically meaningful steady one-dimensional solutions can then be written in the following simple form

$$G > 1 \tag{4.10}$$

and

$$\Delta \geq \frac{\frac{\pi}{2}-\theta_*}{\sqrt{G-1}} \tag{4.11}$$

where

$$\theta_* \equiv \tan^{-1}\left(\frac{G-\rho}{\rho\sqrt{G-1}}\right) \tag{4.12}$$

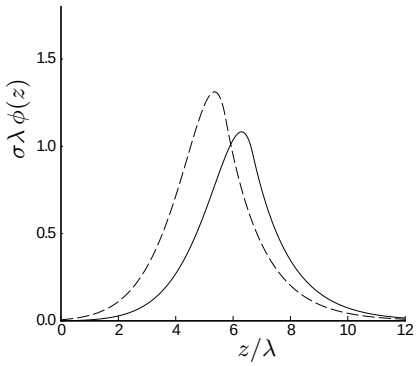

FIGURE 2. Phytoplankton profiles determined by theory, ——— : zero boundary condition, - - - - : no flux boundary condition.

and

$$\rho \equiv 2 + \frac{\lambda}{\Lambda}. \tag{4.13}$$

Figure 1 shows the critical curve in the space of parameters $G - \Delta$. Steady solutions are only possible if conditions are such that the pair of values (G, Δ) characterizing the system lies above the critical curve.

The distribution of phytoplankton with depth is given by

$$\phi(z) = \begin{cases} A_{ep} \exp\left(\frac{z}{\lambda}\right)\left[\sqrt{G-1}\cos\left(\frac{z}{\lambda}\sqrt{G-1}\right) + \sin\left(\frac{z}{\lambda}\sqrt{G-1}\right)\right] & \text{if } z \le H; \\ A_{ap} \exp\left(-\frac{z}{\Lambda}\right) & \text{if } z > H. \end{cases} \tag{4.14}$$

where

$$A_{ep} = \Phi \frac{(G^2 - 2\rho G + \rho^2 G)^{1/2}}{(\lambda\rho + \Lambda G)\sqrt{G-1}\exp\left(\frac{\pi/2 - \theta_*}{\sqrt{G-1}}\right)} \tag{4.15}$$

$$A_{ap} = \Phi \frac{G}{\lambda\rho + G\Lambda} \exp\left[\frac{\lambda}{\Lambda}\frac{\pi/2 - \theta_*}{\sqrt{G-1}}\right] \tag{4.16}$$

and

$$\Phi = \int_0^\infty \phi(z)\, dz \tag{4.17}$$

is the integrated phytoplankton density. The height of the euphotic zone, H, and the integrated phytoplankton density are given by

$$\frac{H}{\lambda} = \frac{\frac{\pi}{2} - \theta_*}{\sqrt{G-1}} \tag{4.18}$$

and

$$\sigma\left(1 + \frac{G\Lambda}{\rho\lambda}\right)\Phi = \frac{\lambda\Delta}{H} - 1. \tag{4.19}$$

The formulation and the analytical solution presented above is a generalization of an analysis by Riley, Stommel & Bumpus (Riley *et al.* (1949)). It differs from this previous work in that the "self-shading" effect introduced through Eq. (4.2) was not considered in the earlier paper. Riley *et al.* considered the depth of the euphotic zone H as fixed.

They then interpreted the eigenvalue equation to mean that a certain relation must exist between the parameters v_p, k_T, r, L, and the depth of the euphotic zone H $(= H_0)$ for solutions to exist. Such a condition, however, seems rather artificial as these parameters assume values independently and only in rare circumstances can they be expected to fall on the curve determined by the eigenvalue equation. The present formulation provides a natural interpretation for the eigenvalue condition. It determines the amplitude of the mode or, equivalently, the integrated phytoplankton density Φ. Riley *et al.* also concluded that for steady non negative solutions, one must have $G > 1$ and the depth of the euphotic zone should *not exceed* a certain critical value. In our formulation, the requirements for physically acceptable solutions are that $G > 1$ and the dimensionless clear water euphotic zone depth $\Delta = H_0/\lambda$ should *exceed* a certain critical value given by (4.11). Unlike the previous analysis which was linear, in our formulation both the amplitude as well as the shape of the depth distribution of phytoplankton are determined because of the nonlinearity introduced in the problem through the self-shading effect.

5. Direct numerical simulation

The analysis presented here is based on a number of simplifying assumptions, not all of which can be expected to hold in natural environments. Measurements of phytoplankton density are available from various sources; however, not all of the parameters needed in the theory may have been measured in a given investigation. Further, interpretation of such data is often complicated by poorly characterized or unknown factors in the physical environment. It would seem reasonable, therefore, to first test the principal results of the analysis by comparing with a "numerical experiment" that is free of all the uncertainties inherent in data from the natural environment. In order to reduce uncertainties arising from the departure from isotropy near the free surface, the simulation is performed for a fast sinking species so that the phytoplankton concentration peaks well below the free surface.

A direct numerical simulation (DNS) is performed in a computational box of aspect ratio $1:1:4$, the depth D being the longest dimension. The velocity field $\mathbf{u}$ is determined by the incompressible Navier-Stokes equations while the phytoplankton density ϕ obeys the evolution equation

$$\frac{\partial \phi}{\partial t} + \mathbf{u} \cdot \nabla \phi = S\phi - v_p \frac{\partial \phi}{\partial z} + k_0 \nabla^2 \phi \tag{5.1}$$

where k_0 is a small "molecular diffusion" coefficient that is introduced to stabilize the calculation by smoothing out any excessively sharp gradients in the scalar iso-surface.

We assume periodic boundary conditions for the velocity $\mathbf{u}$ and pressure p in all three directions. For the scalar ϕ, we assume periodic boundary conditions for the lateral boundaries and zero boundary conditions at the top and bottom surfaces of the box

$$\phi(x, y, 0, t) = 0 \tag{5.2}$$

$$\phi(x, y, D, t) = 0. \tag{5.3}$$

The assumption of periodic boundary conditions at the top and bottom surfaces for the velocity and pressure is chosen for the purpose of this investigation primarily for reasons of simplicity of implementation. It allows us to treat the turbulence as isotropic, consistent with the assumptions in the analytical work. Deviations from isotropy near the free surface are to be expected in a realistic situation, but it is reasonable to undertake a careful investigation of the isotropic case first. The isotropic assumption is rendered

somewhat more plausible if the "upper" boundary is interpreted as an imaginary surface located not at the true free surface, but somewhat below it. Similarly, the "lower" boundary is considered to be an arbitrarily chosen plane well below the euphotic zone where the phytoplankton concentration is essentially zero. The outward flux, F of phytoplankton at the surface $z = 0$ is given by

$$F = -\overline{w\phi} - v_p\overline{\phi} + k_0\overline{\frac{\partial\phi}{\partial z}} \tag{5.4}$$

where the overbar signifies horizontal average. If the layer of water between $z = 0$ and the physical surface is sufficiently thin, phytoplankton production in this layer may be neglected so that a balance prevails between the turbulent transport across $z = 0$ and the flux due to sinking. The appropriate boundary condition for modeling this situation would be

$$F_{z=0} = 0. \tag{5.5}$$

The difficulty of implementing the boundary condition (5.5) is that it provides a constraint on the mean field but not on the fluctuations. Further assumptions about the nonzero Fourier modes of the scalar field need to be introduced for a numerical solution. The only exception to this is the situation where the sinking speed of phytoplankton, v_p, is sufficiently large so that the phytoplankton distribution peaks well below the surface and the surface concentration of phytoplankton is negligible. Here the parameters are chosen to correspond to this situation. In this case, (5.5) may be replaced by (5.2) as a reasonable approximate boundary condition. Further, under these conditions any uncertainties due to possible deviations from isotropy of the turbulent field near the free surface would presumably have a negligible effect on the phytoplankton concentration profile. Since $G \propto 1/v_p^2$ and $\Delta \propto v_p$, $G \to 0$ and $\Delta \to \infty$ as $v_p \to \infty$. In order to remain within the zone of steady solutions in phase space, parameters for the numerical simulation must be chosen so that the point (G, Δ) is in the upper left-hand corner of the parameter space shown in Fig. 1, very close to but above the critical curve.

In order to perform the numerical simulation, an existing pseudospectral code designed for simulating forced isotropic turbulence in the presence of a passive scalar was modified in the following manner to implement the Jassby-Plat model discussed in Section 3. The representation of the scalar field ϕ was changed from Fourier to physical in the z-direction only. The z-derivative operator was changed from spectral to second-order central difference at interior points, reverting to second-order one-sided finite difference at the grid points closest to the boundaries. A scalar field for the light intensity was added and updated at every time step in accordance with the requirements of (3.4) and (3.5). The basic algorithm, which is discussed at length elsewhere (Rogallo (1977)), uses a second-order Runge-Kutta method to execute the time step and uses the phase shift algorithm to dealias. Dealiasing in the z direction was turned off for the scalar field. A grid size of $64 \times 64 \times 256$ was chosen as this seemed to provide a reasonably robust representation of the turbulent field with a well-resolved vertical profile for the mean phytoplankton concentration at a tolerable computational cost. The simulations took about 7.7 seconds per time step on a 650 MHz PC with an Athlon Processor, and the longest run involved $36,000$ steps.

For the numerical experiment, the following parameters were chosen in the Jassby-Plat model (in code units†): $r = 0.1$, $L = 0.18$, $I_0/I_c = 12$, $\mu_0 = 0.05$, $\mu_1 = 0.01$, $v_p = 0.28$,

† That is, these numbers are directly used in the equations with horizontal domain size being 2π. However, all results are presented as dimensionless quantities.

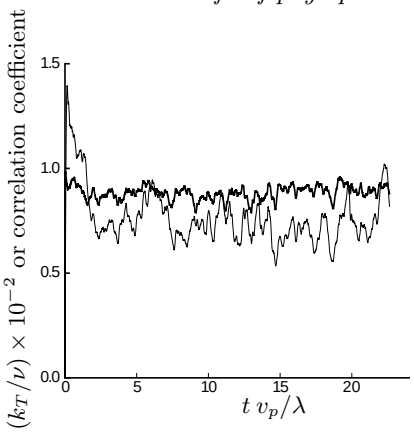

FIGURE 3. The best value of eddy-diffusivity determined by fitting a regression line (———) and correlation coefficient indicating goodness of fit (———) as a function of time.

and, in order that the Jassby-Platt model approximates closely the "Layer Model" a large value was chosen for the parameter α, $\alpha = 10$. The point in the $G - \Delta$ parameter space corresponding to this simulation is indicated in Fig. 1 by the filled circle. The turbulent velocity field was initialized in the usual manner (Rogallo (1977)). The Taylor microscale Reynolds number of the turbulence is $\Re_\lambda \approx 29$, and the Schmidt number is chosen to be $Sc = 0.7$.

The solid line in Fig. 2 is the prediction of the theoretical model presented in Section 4 with a value of the eddy diffusivity that corresponds to that found in the DNS. The theoretical model assumes zero flux at the upper surface while the DNS uses zero concentration. With the parameters chosen, the difference between the solutions using the no flux and the zero boundary conditions is expected to be small. To quantify the degree of dependence of the profile on boundary conditions, we worked out the analytical results corresponding to the $\phi = 0$ rather than the zero flux boundary condition at the upper surface. This solution is very similar to that presented in Section 4. The formulae are omitted for brevity, but the profile corresponding to it is plotted in Fig. 2 as a dashed line. Clearly the two curves are qualitatively similar, but quantitatively the difference is not negligible. The critical curve in parameter space corresponding to the zero boundary condition solution is also depicted in Fig. 1 as a dashed curve. The boundary condition is seen to have a minor impact on the critical curve.

In order to determine the correct value of the diffusivity to use in place of k_T in the analytical results, we perform a linear regression of the form $Y = k_T\, X$ to the data, where $X = (\partial\overline{\phi}/\partial z)$ and $Y = -\overline{w\phi}$. The slope of the regression line then gives k_T. Figure 3 shows the time history of the regression line slope, k_T, together with the correlation coefficient characterizing the goodness of the fit. The average value of k_T was determined by time averaging the data after the initial transient, i. e. for $tv_p/\lambda > 5$. This value is augmented slightly by the small "molecular" diffusivity k_0 for use in computing the analytical profiles.

In order to test the stability of the solution numerically and also to test that the profile indeed does evolve towards a steady state, we started the simulation from an initial condition well below the theoretical prediction. The initial phytoplankton profile was arbitrarily chosen as a "sine to the fourth" distribution with an amplitude of about 10 percent of that expected from the theory. In Fig. 4 the lines show concentration profiles

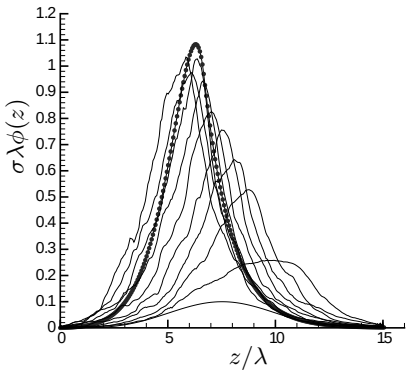

FIGURE 4. The time evolution of the horizontally averaged plankton concentration as a function of depth, the symbols represent the theoretically predicted profile.

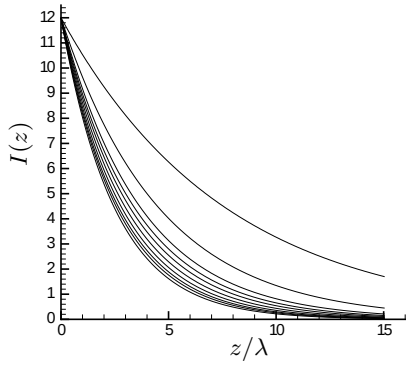

FIGURE 5. The time evolution of the light intensity as a function of depth; the highest curve is the initial profile.

evolving from this initial condition and approaching the theoretical profile depicted by the symbols. The "self-shading" effect is obvious in Fig. 5, which contains the evolution of the light intensity. As the phytoplankton concentration increases, the light reaching any given layer decreases, resulting in a decreased rate of production.

As a final test, we performed another simulation using the theoretical profile with the zero concentration boundary condition at the surface. However, we reduced the growth rate to $r = 0.05$, corresponding to the point depicted by the open circle in the parameter space in Fig. 1. Since this is below the critical curve, it is expected the the phytoplankton profile would decay away. This is indeed what is observed. Figure 6 shows the decay of the depth integrated phytoplankton concentration density Φ as a function of time.

These are preliminary results. It is not yet clear that the distributions have reached a statistically stationary state. The results of more detailed investigations will be presented at a future date.

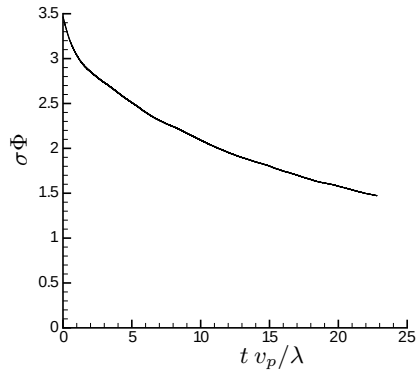

FIGURE 6. The time evolution of the depth integrated plankton concentration showing the decay of a healthy population when the operating point $(G,\,\Delta)$ lies below the critical curve.

6. Conclusion & future plans

Biology and geophysical phenomena are intricately interconnected and are merely two essential components of a vast and complex machinery that operates on the planetary scale. This complexity starts to become comprehensible only if we view it through the lens of a highly simplified model that captures only the essential and then add in the details as successive refinements when comparison with data warrants it. The present paper represents merely a first step in this incremental process.

A general conclusion that may be drawn from the comparison of the numerical simulations and the theory is that an eddy diffusivity model for turbulent transport appears to be adequate for the purpose of predicting the mean concentration of organisms. Also, the simulations seem to indicate that the solution corresponding to the analytical profile is globally stable in the appropriate region of parameter space. Below the critical curve, the zero solution seems to be globally stable. This conclusion, however, is tentative as it is based on a very limited number of simulations.

The most serious shortcoming of the present model is that it applies only in eutrophic environments. A natural extension of the model would be the introduction of the dynamics of nutrients into the model. A certain formal similarity of the mathematics of plankton dynamics with that of combustion is obvious (both are reaction-diffusion systems). Carrying this analogy further, the distinction between eutrophic and oligotrophic environments is not unlike the distinction between "premixed" and "diffusion flames" (the latter being dominated by the depletion of reactants, similar to depletion of nutrients in the case of plankton dynamics).

The second critical constraint is the implicit assumption that the entire water column is uniformly turbulent. In many lakes the onset of warmer conditions during spring causes the water column to become stably stratified so that the wind driven turbulence cannot penetrate to very deep layers. The change in the relative position of the turbocline with respect to the boundary of the euphotic zone due to stratification effects brought about by thermal and salinity gradients is a very important component of phytoplankton dynamics. In particular, the classical Sverdrup Critical Depth Model (SCDM), which is supported by a wide range of geophysical data, correlates phytoplankton blooms with the turbocline becoming shallower than a certain critical depth. Generalization of the current model would be necessary to include these very important effects.

The current model assumes the plankton distribution to be statistically homogeneous in the horizontal directions. This simplified model fails to throw any light on the rich and varied horizontal structure seen in satellite images of the plankton distribution in natural waters. Phytoplankton patches are transported by horizontal currents, but they can also be expected to show intrinsic dynamics. For example, if a small patch of phytoplankton are introduced in waters for which the point (G, Δ) in parameter space is favorable to phytoplankton growth, what are the dynamics of the process by which the steady state distribution in the above model gets established? The solution is likely to be analogous to the problem of the propagation of an ignition front leading to the formation of a flame sheet. The details of such processes for the phytoplankton system are poorly understood and would be interesting areas for future investigations.

Acknowledgments

We are indebted to Professors J. E. Koseff, J. Jimenez, and R. M. Alexander for bringing some valuable references to our attention. Professor Alexander's very enjoyable book (Alexander (1992)) was an important source of inspiration for this work.

REFERENCES

Alexander, R. M. 1990 Size, speed and buoyancy adaptations in aquatic animals. *Amer. Zool.* **30**, 189.

Alexander, R. M. 1992 *Exploring Biomechanics: Animals in motion.* Scientific American Library.

Charlson, R.J., Lovelock, J. E., Andreae, M. O. & Warren, S. G. 1987 Oceanic phytoplankton, atmospheric sulphur, aloud albedo and climate. *Nature.* **326**, 655.

Edwards, A. M. & Brindley, J. 1999 Zooplankton mortality and the dynamical behavior of plankton population models. *Bull. Math. Biol.* **61**, 303.

Eppley, R. W., Holmes, R. W. & Strickland, J. D. W. 1967 Sinking rates of marine phytoplankton measured with a fluorometer. *J. Exp. Mar. Biol. Ecol.* **1**, 191.

Fenchel, T. 1974 Intrinsic rate of natural increase: the relationship with body size. *Oecologia.* **14**, 317.

Gibson, C. H. 2000 Laboratory and ocean studies of phytoplankton response to fossil turbulence. *Dynamics of atmospheres and oceans.* **31**, 295.

Jassby, A. D. & Platt, T. 1976 Mathematical formulation of the relationship between photosynthesis and light for phytoplankton. *Limnol. Oceanogr.* **21**, 540.

Jimenez, J. 1997 Oceanic turbulence at millimeter scales. *Scientia Marina.* **61**, Suppl. 1, 47. ["Lectures on plankton & turbulence", ed. Marrase, C., Saiz, E. & Redondo, J. M."]

Koseff, J. R., Holen, J. K., Monismith, S. G. & Cloern, J. E. 1993 Coupled effects of vertical mixing and benthic grazing on phytoplankton populations in shallow, turbid estuaries. *J. Marine Res.* **51**, 843.

Lucas, L. V., Cloern, J. E., Koseff, J. R., Monismith, S. G. & Thompson, J. K. 1998 Does the Sverdrup critical depth model explain bloom dynamics in estuaries? *J. Marine Res.* **56**, 375.

Lucas, L. V., Koseff, J. R., Cloern, J. E., Monismith, S. G. & Thompson, J. K. 1999 Processes governing phytoplankton blooms in estuaries. I: The local production-loss balance. *Marine Ecology Progress Series.* **187**, 1.

Lucas, L. V., Koseff, Monismith, S. G., Cloern, J. E. & Thompson, J. K. 1999

Processes governing phytoplankton blooms in estuaries. II: The role of horizontal transport. *Marine Ecology Progress Series.* **187**, 17.

Margalef, R. 1978 Life-forms of phytoplankton as survival alternatives in an unstable environment. *Oceanological Acta.* **1**, 493.

Peters, F. & Marrase, C. 2000 Effects of turbulence on plankton: an overview of experimental evidence and some theoretical considerations. *Marine Ecology Progress Series* (in press).

Reynolds, C. S. 1984 *The ecology of freshwater phytoplankton.* Cambridge University Press.

Riley, G. A., Stommel, H. & Bumpus, D. F. 1949 Quantitative ecology of the plankton of the western north atlantic. *Bull. Bingham Oceangr. Coll.* **XII**(3), 1.

Rogallo, R. 1977 An ILLIAC program for the numerical simulation of homogeneous incompressible turbulence. *NASA Tech. Mem.* **NASA TM-73203**.

Sverdrup, H. U., Johnson, M. W. & Fleming, R. H. 1946 *The Oceans Their Physics, Chemistry, and General Biology.* Prentice Hall.

Sverdrup, H. U. 1953 On conditions for the vernal blooming of phytoplankton. *J. Conseil Exp. Mer.* **18**, 287.

Thurman, H. V. 1997 *Introductory Oceanography, 8th edition* Prentice Hall.

Truscott, J. E. & Brindley, J. 1994 Ocean plankton populations as excitable media. *Bull. Math. Biol.* **56**(5), 981.